

Article

Experimental and Photothermal Performance Evaluation of Multi-Wall Carbon-Nanotube-Enhanced Microencapsulation Phase Change Slurry for Efficient Photothermal Conversion and Storage

Changling Wang^{1,2,3,*}, Guiling Zhang^{1,2,3} and Xiaosong Zhang^{1,2,3}¹ School of Energy and Environment, Southeast University, Nanjing 210016, China² Engineering Research Center of Building Equipment, Energy, and Environment, Ministry of Education, Nanjing 210106, China³ Shenzhen Research Institute, Southeast University, Shenzhen 518000, China

* Correspondence: 230169639@seu.edu.cn; Tel.: +86-188-5117-5256

Abstract: Melamine formaldehyde was used as the shell material and n-eicosane as the core material with the method of in situ polymerization to synthesize microencapsulated phase change materials (MPCMs). To enhance the thermophysical characteristics and photothermal conversion performance of the MPCM slurry, multi-wall carbon nanotubes were added, and the microscopic morphology and thermophysical parameters of the MWCNT-MPCM slurry were analyzed. The thermal conductivity, viscosity, and photothermal conversion properties of the slurry were examined. The results indicated that the synthesized MPCMs were nucleated and unbroken, with a spherical form and a latent heat of phase transition of up to 135.92 kJ/kg. The MPCM was stable when dispersed in water, and its thermal conductivity rose with the temperature but slightly decreased during the phase transition period. The viscosity rose with the addition of the MPCM, with a jump at 20% MPCM content. The addition of MWCNTs had a minor effect on the material's thermophysical properties. The thermal conductivity increased from 0.55 W/m·°C to 0.6 W/m·°C when MWCNTs were added to the material. The viscosity of a 20% MPCM slurry exceeded 3000 mPa·s when 0.5% MWCNTs were introduced. Under 1 sun of sunlight, the mixture's peak temperature could reach 60 °C at 0.5% MWCNT concentration. The MWCNT-MPCM slurry is capable of producing efficient solar photothermal conversion without sacrificing other thermophysical properties, and it has several applications in solar energy consumption and thermal engineering.

Keywords: microencapsulated phase change materials; solar energy; photothermal conversion; in situ polymerization



Citation: Wang, C.; Zhang, G.; Zhang, X. Experimental and Photothermal Performance Evaluation of Multi-Wall Carbon-Nanotube-Enhanced Microencapsulation Phase Change Slurry for Efficient Photothermal Conversion and Storage. *Energies* **2022**, *15*, 7627. <https://doi.org/10.3390/en15207627>

Academic Editors: Pedro Dinis Gaspar, Pedro Dinho da Silva and Luis C. Pires

Received: 5 September 2022

Accepted: 12 October 2022

Published: 15 October 2022

Publisher's Note: MDPI stays neutral with regard to jurisdictional claims in published maps and institutional affiliations.



Copyright: © 2022 by the authors. Licensee MDPI, Basel, Switzerland. This article is an open access article distributed under the terms and conditions of the Creative Commons Attribution (CC BY) license (<https://creativecommons.org/licenses/by/4.0/>).

1. Introduction

As a result of the rapid expansion of the world economy, a growing number of people are becoming concerned about the impending energy crisis and the deterioration of the environment that will result from the continued use of fossil fuels. The 17 Sustainable Development Goals (SDGs) were agreed upon by all nations that are members of the United Nations as part of the Paris Agreement in 2015. In order to fulfil the CO₂ reduction objective, set out in the Paris Agreement for the year 2015, there is an unavoidable requirement that fossil fuel use should be dropped to 20%. The transition to energy sources with low carbon emissions is vital as fossil fuels are responsible for two-thirds of all greenhouse gas emissions [1]. Solar energy is the only source of energy that is both renewable and free of carbon emissions, and it is the only source that has the potential to replace fossil fuels on a sufficiently large scale [2–5]. Given the fact that solar energy is both intermittent and discontinuous, its distribution in time and place is also unequal. This mismatch between

supply and demand is a significant barrier to the development of solar energy applications. Converting solar energy into thermal energy and storing it has been proven to be an effective method of collecting and storing solar energy. Researchers are eager to find out more about phase change materials owing to the potential they hold for thermal storage applications thanks to their high thermal storage capacity and consistent phase change temperature range [6].

As organic phase change materials undergo phase separation less regularly than inorganic phase change materials, they exhibit better stability. The organic phase change material is not appreciably subcooled, so the phase change temperature is essentially constant. This phase change material is nontoxic and does not induce subcooling; as a result, it is appropriate for use in commercial applications and has won the attention of a great number of researchers [3]. When they are in their liquid state, organic phase change materials exhibit a high degree of fluidity. This is typical of many other types of solid–liquid PCMs as well. This is regarded as a disadvantage of solid–liquid PCMs, as they not only lead to basic handling challenges but also to leakage, penetration, and loss during usage. Other drawbacks include increases in volume during phase transitions, poor thermal conductivity, supercooling, corrosion, evaporation, and chemical degradation. Because of these issues, the thermophysical properties of phase change materials are often considerably diminished, and their prospective applications are severely hampered [7].

There have been several advances over the years in the ways of enhancing the durability of phase change materials and making them more user-friendly. Microencapsulated phase change materials (MPCMs) are of special interest to researchers as they may efficiently tackle the issues of leakage, evaporation, and diffusion of phase change materials that occur throughout the energy storage process [8,9]. Microencapsulated phase change materials are produced by encapsulating the phase change material inside a more robust shell material, which keeps the core material within after the phase change has occurred. Yuan et al. designed bilayer organic phase change microcapsules by utilizing n-eicosane as the PCM, melamine formaldehyde (MF) as the shell layer, and polydopamine as the outer coating to enhance the effectiveness of photothermal energy conversion of the microcapsules [10]. Al-shannaq et al. produced a MPCM by using polymethyl methacrylate for the shell, paraffin for the core, and pentaerythritol tetra acrylate as the crosslinker. The microcapsules made with this approach had a much higher PCM percentage, and the particle size of the microcapsules could be minimized by utilizing a surfactant combination [11]. Sun et al. produced a microencapsulated phase change material, with n-octadecane as the core material and silica as the shell material in a process called microemulsion interfacial polycondensation. With the aid of electrostatic self-assembly, the BN was successfully immobilized on the silica shell [12]. Using paraffin as the PCM and chitosan/carboxymethyl cellulose as the capsule shell, Chen et al. constructed phase change microcapsules, and obtained phase change microcapsule gypsum by introducing it directly as a hydrogel during the gypsum manufacturing process. The findings demonstrated that phase change microcapsules could increase the thermal inertia of the plaster and maintain a lower inner temperature [13]. Zhu et al. synthesized MPCM via an interfacial polymerization technique. The core ingredient was n-octadecane and the shell material was polyurea. This MPCM was subsequently used to wall panels. As shown by the experiments, this thermal storage coating may improve the indoor thermal environment and, hence, the occupants' comfort [14]. MPCMs are a great thermal storage option. The development of materials with enhanced photothermal conversion properties is crucial due to pure phase change materials' poor white light absorption [6].

As they are nanosized and have an excellent thermal conductivity, nanomaterials potentially contribute to the transfer of heat. Simultaneously, some nanoparticles have excellent light absorption and might even conduct quick photothermal conversion; the combination of nanomaterials and phase change materials holds significant promise for the advancement of photothermal conversion and energy storage [15]. Carbon nanomaterials, metal nanomaterials, and nonmetallic nanomaterials have been used by researchers

to improve the efficiency of photothermal conversion [16–19]. Lin et al. incorporated light-absorbing carbon nanotubes into a complex composed of expanded graphite and paraffin wax. According to the research, this composite phase change material not only exhibited a high thermal conductivity but also a high capacity for solar energy absorption [20]. Zheng et al. used a copper foam substrate that included graphene aerogel and encapsulated paraffin as the PCM. Experiments in photothermal conversion demonstrated the material's exceptional photothermal conversion capabilities, showing the material's promise for photothermal conversion and storage [21]. Maithya et al. developed phase change microcapsules by using the Pickering suspension polymerization method. The n-eicosane was selected as the PCM core, while polyurea served as the cladding material. Graphene oxide was used as a colloidal stabilizer [22]. Maithya et al. continued their study on Pickering emulsion polymerization thereafter. Maithya et al. employed bio-regenerated chitin obtained from shrimp shells as a Pickering emulsifier in the manufacture of polyurea/paraffin microencapsulated phase change materials. As a photon trap, graphene oxide was incorporated into the design. The material parameters and the efficiency of the photothermal conversion were analyzed [23]. Additionally, Zhao et al. created phase change microcapsules with Pickering emulsions using graphene as the Pickering stabilizer. Paraffin served as the PCM within the microcapsules, whereas MF formed the shell. Thermophysical characteristics and the effectiveness of photothermal conversion of phase change microcapsules were investigated. Concentrations of graphene and core-shell ratios were two variables studied in detail [24]. Liu et al. employed Fe₃O₄ nanoparticles to increase the photothermal conversion performance of phase change microcapsules and demonstrated a 47.9% improvement in photothermal conversion efficiency [25]. Fan et al. created phase change microcapsules using n-dodecane as the core material and titanium dioxide as the shell material, and then coated them with graphene oxide-copper sulfide to achieve full spectrum conversion and solar energy storage [26]. In addition, various theoretical and simulation investigations on nanomaterials for solar energy conversion performance have been conducted [27–31].

Researchers have focused a lot of their attention on carbon nanomaterials, particularly carbon nanotubes, owing to the exceptional thermal property and photothermal conversion capabilities [1]. Hu et al. provided a flexible phase change composite by using a cross-linked interpenetrating network of CNTs and styrene-butadiene-styrene packed with paraffin wax. The results revealed that these composite phase change materials might be used for the thermal control of electronic devices and solar thermal storage [32]. Atinafu et al. used a one-step hydrothermal method to produce a shape-stabilized phase-change material. They employed bamboo charcoal as the framework and n-dodecane as the phase change material (PCM). Additionally, CNTs were added to improve the thermophysical properties of the material. The results revealed that this material retained its shape and had a high latent heat load, making it appropriate for thermal management and thermal energy storage applications [33]. Ong et al. employed polyurethane acrylic paint and a curing agent to bind CNTs to a microencapsulated phase change material shell. The results indicated that this layer of carbon nanotubes could increase the total thermal conductivity without impairing phase change performance [34].

In addition, there are several review articles that provide a comprehensive summary of microencapsulated phase change materials. With the help of these articles, we are able to obtain a more in-depth understanding of the applications of microencapsulated phase change materials and with nanomaterials in a variety of fields. Khudhair et al. presented an overview of an early approach for the microencapsulation of phase change materials and showed that PCM may be associated with other materials more easily via the encapsulation process, allowing for a considerably broader range of dispersion and application. The findings of this review indicate that microencapsulated phase change materials have received relatively little investigation in the field of solar photothermal conversion [35]. Tyagi et al. performed a comprehensive review of microencapsulated phase change materials in their work. This report examined a discussion of preparation methods, materials,

and applications. It is plainly clear that microencapsulated phase change materials are not yet used extensively in the area of solar energy [36]. Giro-Paloma et al. provided a comprehensive summary of the various types of microencapsulated phase transition materials, as well as their manufacturing and characterization techniques. A collection of applications of microencapsulated phase change materials was provided. This research also indicated that viscosity and thermal conductivity are crucial factors for MPCMs; however, the review did not seem to address much this element of the study [37]. Yu et al. examined current advancements in the use of phase change materials in photovoltaic/thermal systems. They discovered that the incorporation of multi-wall carbon nanotubes into water or phase-change materials could boost the thermal conductivity of the materials. On the other hand, it is evident that research into the utilization of carbon nanotube materials for photothermal conversion and storage has not been nearly as extensive [38]. Tang et al. summarized current advancements in the area of photo-response conversion of phase change materials. They emphasized that carbon nanotubes are very promising for photothermal conversion. According to this study's summary, research combining carbon nanotubes and phase change microcapsules for photothermal conversion is rare [39]. According to various reviews, despite the urgency and potential of investigating multi-wall carbon nanotubes in conjunction with phase change microcapsules for photothermal conversion, research in this field has yet to develop [40–43].

In this study, microencapsulated phase change materials (MPCMs) were prepared using in situ polymerization. The microcapsules' core was n-eicosane, whereas the shell was polymethyl methacrylate. Multi-wall carbon nanotubes (MWCNTs) were also added to a MPCM slurry to improve the thermal and photothermal conversion capabilities. The microscopic morphology, thermal properties, chemical structure, stability, thermal conductivity, viscosity, and photothermal conversion performance of the MWCNT-MPCM were examined using scanning electron microscopy (SEM), differential scanning calorimeter (DSC), Fourier transform infrared spectroscopy (FTIR), transient hot-wire theory, a viscometer, and a homemade photothermal conversion device.

2. Materials and Methods

2.1. Material

The n-eicosane as a phase change material was purchased from Macklin Reagent (Shanghai, China). SDS (Aladdin, Shanghai, China), Span80 (Yuanye Bio-Technology, Shanghai, China), and Tween80 (Aladdin, Shanghai, China) were used as compounding emulsifiers. Melamine (Sigma, Shanghai, China) and formaldehyde solution (37 wt.%, Aladdin, Shanghai, China) were used to prepare shell monomers for microencapsulation. To modify the pH and induce nucleation, triethyl-aminol (Sigma, Shanghai, China), ammonium chloride (Macklin, Shanghai, China), and glacial acetic acid (Merck, Shanghai, China) were utilized. The ethanol was provided by Macklin (Shanghai, China). The purchased reagents were not further purified throughout the experiment.

Multi-wall carbon nanotubes (MWCNTs) and a Dispersant for Carbon nanotube aqueous solutions (CNT-DASs) were purchased from Nanjing XFNANO Materials Tech Co., Ltd. (Nanjing, China). Deionized water was home-made in the laboratory.

2.2. Synthesis of Microencapsulated Phase Change Materials

The in situ polymerization was used to make the phase change microcapsules, which included n-eicosane as the phase change material and melamine formaldehyde resin as the shell material. A compounded emulsifier was used in the preparation process. To make the compounded emulsifier, SDS, Span80, and Tween80 were blended with water in a certain ratio. The schematic diagram of the preparation of the MPCM is shown in Figure 1. The emulsion synthesis was performed in a 100 mL three-neck jacketed flask with a mechanical stirring mechanism, and the reaction temperature in the flask was regulated by circulating water via an external thermostat tank. Amounts of 6 g of n-eicosane, 2 g of compound emulsifier, and 60 mL of deionized water were added and stirred at 1000 rpm/min for

60 min at 40 °C, followed by emulsifying at 8000 rpm/min for 10 min using a high-speed shear mixer. The pH was adjusted to 4.5 to 5.0 using a 10 wt.% glacial acetic acid solution.

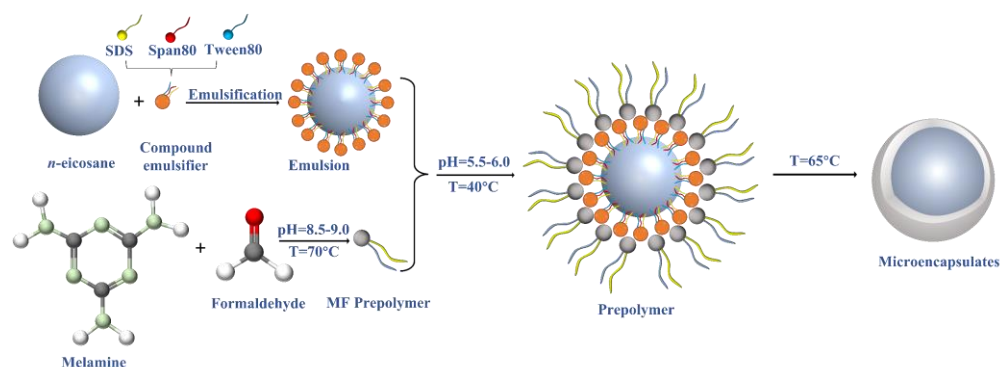


Figure 1. Schematic diagram of the preparation of MPCM.

In a 150 mL three-neck flask, 5 g of melamine, 25 mL of formaldehyde solution (37%), and 20 mL of deionized water were mixed. The pH was adjusted to 8.5–9.0 using 10% triethanolamine. The mixture was agitated at 70 °C for 60 min to generate the prepolymer solution.

The prepolymer was added dropwise into the emulsion at 360 rpm/min with stirring at 40 °C. The pH was adjusted to 5.5–6.0 using ammonium chloride solution and gradually heated to 65 °C. Then, the glacial acetic acid solution was used to adjust the pH to 3.5–4.0, was continued to stir for 2 h, and was lowered to room temperature. The samples were washed with deionized water and anhydrous ethanol and dried in a vacuum drying oven at 50 °C for 24 h.

2.3. Preparation of the Nano-Enhanced MPCM Slurry

Four different mass fractions of the MPCM water slurry (5% to 20%) were combined with four different mass fractions of nanoparticle water dispersions (0.2% to 0.5%). At room temperature, deionized water and MWCNTs were first combined, and then the CNT-DAS was added to the resulting solution. The mixture was magnetically stirred at 500 rpm for 30 min and then dispersed over the course of 120 min with a 900 W ultrasonic processor. A jacketed beaker was linked to cold water at a constant temperature to prevent deactivation of the dispersant above 40 °C. A specific proportion of MPCM was added into the MWCNT mixture and stirred magnetically at 600 rpm for 60 min to produce a MWCNT-MPCM slurry.

2.4. Characterization and Measurement

Scanning electron microscopy (Helios 5 CX, ThermoFisher Scientific, Waltham, MA USA) was used to observe the surface morphology of the MWCNTs, MPCM and MWCNT-MPCM. Carbon nanotubes, phase change microcapsules, and dried nano-enhanced phase change microcapsules were analyzed using a Fourier-transform infrared spectrophotometer (FTIR, ThermoFisher Scientific). A micro-calorimeter (μ DSC7 Evo, SETARAM Instrumentation) was used to determine the latent heat of phase change and the phase change temperature zone of samples. The temperatures tested varied from 5 °C to 65 °C with a 1.2 °C/min heating rate. The instantaneous hot wire method (TC3000E, Xiayi, China) was used to test the thermal conductivity of materials. The sample was put in a jacketed beaker linked to a constant-temperature water bath to guarantee a consistent temperature during the test. The samples were put in two constant-temperature water baths at 0 °C and 60 °C and cycled 10 times to assess the samples' thermal cycling stability. The materials were evaluated for photothermal characteristics utilizing a laboratory-built solar collector test set (Figure 2). As the simulated light source, a xenon lamp with adjustable optical power (CEL-PE300L-3A, Beijing China Education Au-Light Co., Ltd., Beijing, China) was used. The solar simulator power was held constant throughout the test, and the irradiation intensity of the

sample's effective collector plane was set to 1 solar intensity. In this study, the effective collection plane was placed at the liquid level of the sample. The viscosity of the slurry was measured using a digital viscometer (SNB-1, Hengping, China, range: $0.1\text{--}1 \times 10^5$ mPa·s) with four speeds (6 rpm/min, 12 rpm/min, 30 rpm/min, and 60 rpm/min) to minimize mistakes caused by the shear rate.

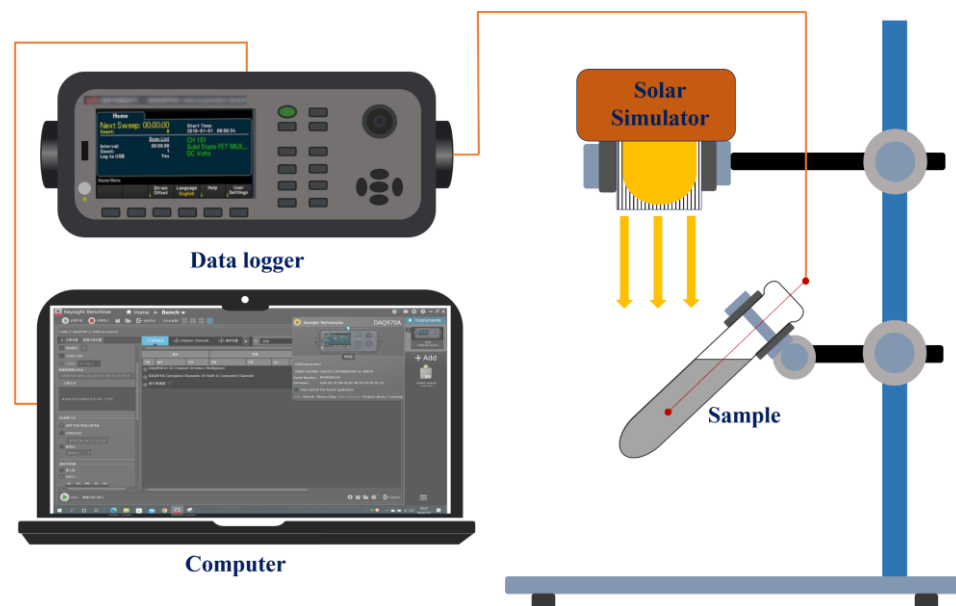


Figure 2. Schematic diagram of solar collector test set.

3. Results and Discussion

Characterization

The microscopic morphology of multi-wall carbon nanotubes, microencapsulated phase change materials, and nano-enhanced microencapsulated phase change materials were revealed by scanning electron microscopy. The MWCNTs have an outside diameter of roughly 50 nm and a length ranging from 0.5 μm to 2 μm (Figure 3a). The microcapsules in the SEM field of view in Figure 3b are all well coated and do not shatter. The particle size distribution plot (Figure 3f) demonstrates that most of the microcapsules have particle sizes ranging from 1 μm to 4 μm , with 2 μm particle sizes the most observed. The microscopic morphology of the nano-enhanced phase change microcapsules is shown in Figure 3c. The preparation process has no influence on the phase change microcapsules' microstructural integrity, MWCNTs are uniformly distributed on the shell surface of the phase change microcapsules, and the greater length of MWCNTs forms a heat conduction pathway between the phase change microcapsules. The prepared materials were mixed with deionized water to make the aqueous dispersions, and Figure 3d depicts digital pictures of the samples, the MPCM slurry, MWCNT slurry, and MPCM/MWCNT slurry, from left to right. The appearance of the MPCM/MWCNT slurry in the figure is not significantly different from the pure MWCNT slurry. After standing for 12 h, no considerable delamination occurs among these samples except the 20% MPCM.

The thermal characteristics of the MPCM alter very little before and after the addition of MWCNTs, according to DSC measurements (Figure 3e), and the complete findings are provided in Table 1. It should be emphasized that each sample was cycled three times, with the results averaged. Figure 3g shows that the temperature profile of the MWCNT-MPCM slurry remains steady after 10 heating/cooling cycles, showing the prepared sample's reliable thermal stability. Figure 3h depicts the density of the MPCM slurry at various MPCM concentrations. The density of the MPCM slurry declines with increasing MPCM content, reaching 992 kg/m³ when the concentration is raised to 40%.

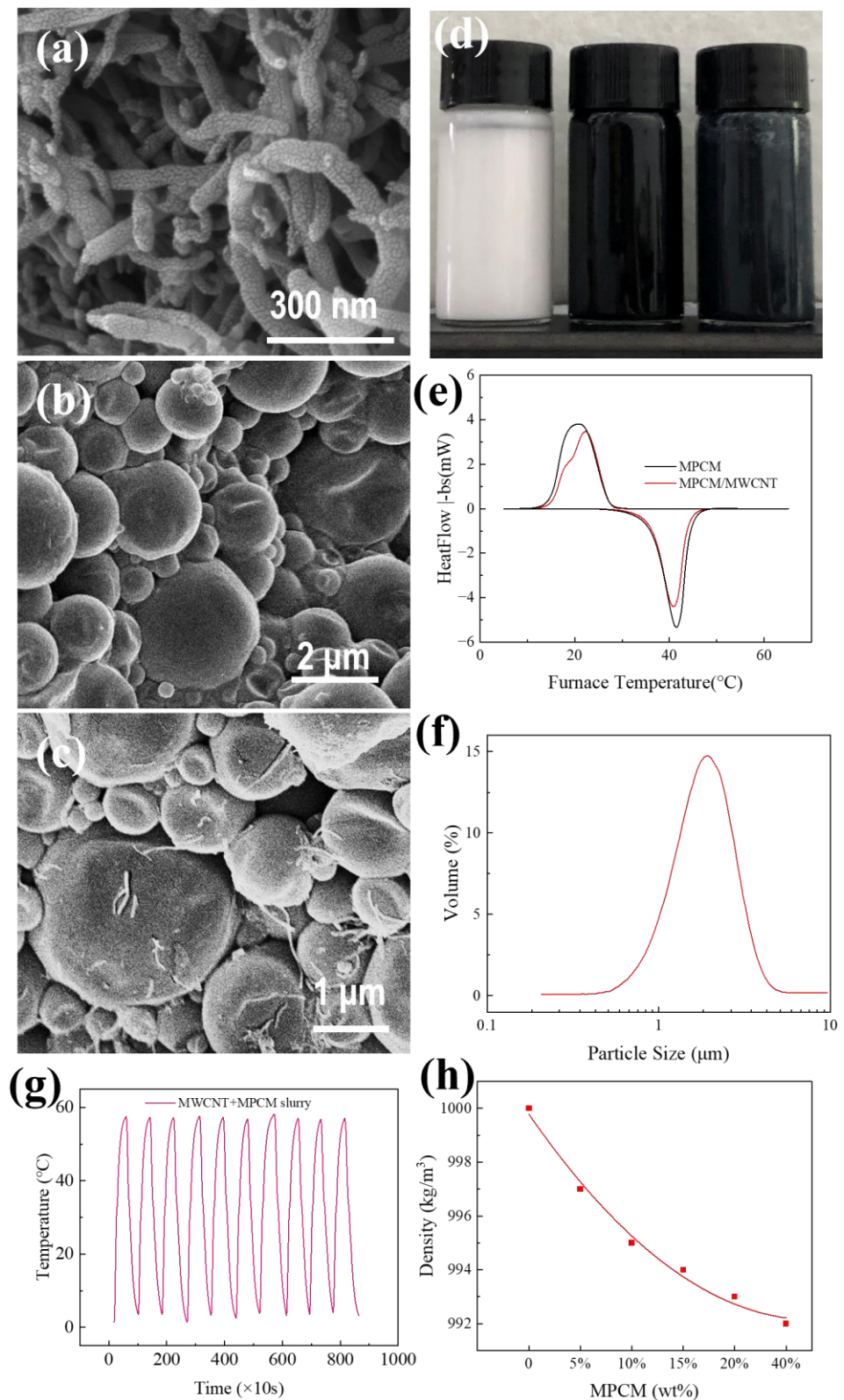


Figure 3. SEM: (a) MWCNT, (b) MPCM, and (c) MWCNT-MPCM; (d) digital images of MPCM slurry, MWCNT water dispersion, MWCNT-MPCM slurry (from left to right), (e) DSC curves, (f) particle size distribution of MPCM, (g) thermal cycle test, and (h) density.

The chemical composition of the phase change microcapsules was determined using FTIR measurements, and the findings are displayed in Figure 4. The absorption peak near

3347 cm^{-1} for the MPCM indicates a superposition of O-H and N-H stretching vibrations. C-H peaks of n-eicosane appear at 2957 cm^{-1} , 2923 cm^{-1} , 2849 cm^{-1} , and 1468 cm^{-1} . The -C=N- vibration in the plane of the triazine ring system is represented by the absorption peak around 1563 cm^{-1} . The -CH₃ group's C-H bending vibration is represented by 1468 cm^{-1} . The stretching vibrations of C-N and C-O are connected to the absorption peaks at 1128 cm^{-1} and 1030 cm^{-1} . The stretching vibration of the triazine ring at 811 cm^{-1} is the MF resin's signature peak. The in-plane stretching vibrations of more than four -CH₂-continuous groups are responsible for the absorption peak around 723 cm^{-1} . MPCM spectra are quite similar before and after MWCNT insertion. This demonstrates that carbon nanotubes have no influence on the chemical structure of phase change microcapsules.

Table 1. DSC data of MPCM and MWCNT-MPCM.

Properties	MPCM	MWCNT-MPCM
Melting onset temperature ($^{\circ}\text{C}$)	36.19	36.24
Melting offset temperature ($^{\circ}\text{C}$)	44.36	43.77
Melting peak temperature ($^{\circ}\text{C}$)	41.41	40.87
Solidifying onset temperature ($^{\circ}\text{C}$)	26.88	27.26
Solidifying offset temperature ($^{\circ}\text{C}$)	14.99	14.57
Solidifying peak temperature ($^{\circ}\text{C}$)	20.25	22.30
Latent heat-melting (kJ/kg)	135.92	107.72
Latent heat-solidifying (kJ/kg)	139.79	111.41

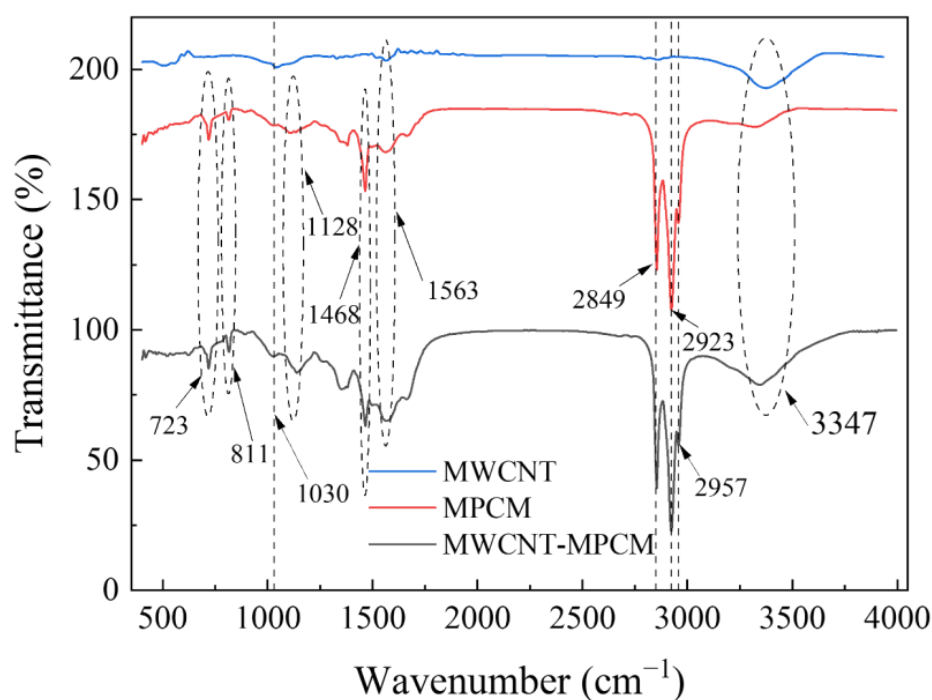


Figure 4. FTIR spectra of MWCNT, MPCM, and MWCNT-MPCM.

The MWCNTs and MPCM were mixed in a specific ratio with deionized water to prepare the MWCNT water dispersion and MPCM slurry. The thermal conductivity of the samples was tested using the transient hot wire method. In order to avoid the generation of natural convection, this study shortened the acquisition time to 1 s and examined the temperature rise time log curve at the end of each test to ensure no natural convection occurred. Figure 5 depicts the thermal conductivity at various temperatures. Overall, thermal conductivity increases as the temperature increases. The thermal conductivity of the 0.5% MWCNT water dispersion can reach 0.76 $\text{W}/\text{m}\cdot^{\circ}\text{C}$ at 50 $^{\circ}\text{C}$, which is significantly greater than that of water (Figure 5a). It is shown that the thermal conductivity of the MWCNT

water slurry increases with the addition of carbon nanotubes, and the thermal conductivity of 0.4% and 0.5% MWCNTs is higher than that of pure water at every temperature. This is mainly because evenly dispersed MWCNTs in water form a heat transfer bridge, improving the thermal conductivity of the dispersion. When the addition of nanomaterials is minimal, the thermal conductivities for the samples of 0.2 and 0.3% MWCNTs are comparable or lower than for water. The MWCNTs do not establish a thermally conductive channel between themselves with low concentration. This is consistent with the explanation of the approach in Figures 6 and 7. In addition, the surfactants used to improve the slurry's stability have the effect of decreasing its thermal conductivity. There is also a minor change in the observed thermal conductivity of the MWCNT water dispersion after the temperature exceeds 41.8 °C. The fluctuations in the results are primarily attributable to irregular thermal movements within the liquid as the temperature rises. However, these fluctuations do not alter the fundamental rule that the thermal conductivity of a liquid increases as the temperature rises. Figure 5b illustrates the thermal conductivity values of different MPCM slurry concentrations. The apparent thermal conductivity drops in the phase change region due to the phase transition of the MPCM, and the reduction rises with increasing MPCM concentration. The thermal conductivity of the MPCM slurry decreases with increasing concentration. Before the phase transition, the thermal conductivity of the slurry with 5% concentration is close to about 0.6 W/m·°C, while the thermal conductivity of the slurry with 20% concentration is only about 0.5 W/m·°C. The lower thermal conductivity of the MPCM slurry compared to water is mainly due to the low thermal conductivity of both the MF shell and the internal n-eicosane core. Furthermore, no effective heat conduction channel exists between the phase change microcapsules (Figure 7). Another noticeable difference between the MPCM slurry and MWCNTs is that the thermal conductivity of the MPCM slurry rarely fluctuates in the high-temperature region, due to the higher viscosity of the MPCM slurry and lower thermal convection. The viscosity characteristics of the MPCM slurry is examined in detail in the next section.

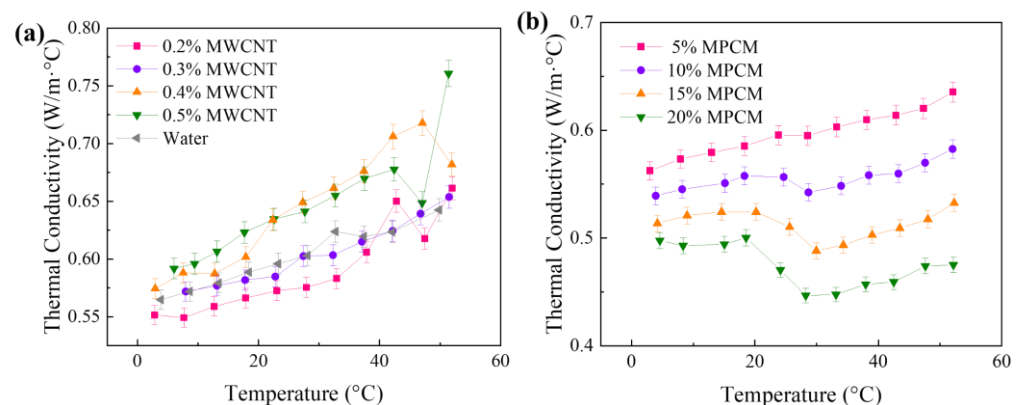


Figure 5. Thermal conductivity in various temperatures: (a) MWCNT water dispersion and (b) MPCM slurry.

Figure 6 depicts the thermal conductivity of the mixture after combining a low quantity of MWCNTs and MPCM. The addition of MWCNTs improves the thermal conductivity considerably. Using a 5% MPCM slurry as an example, the thermal conductivity could well be enhanced from 0.55 W/m·°C to 0.61 W/m·°C following the addition of 0.5% MWCNTs. When MWCNTs are added at 0.2%, there is no benefit on the thermal conductivity improvement. This is mostly because, while MWCNTs have a high thermal conductivity, the extremely little added quantity cannot construct a full thermal conductivity channel. When the amount of MWCNTs applied grows, the most sufficient MWCNTs develop thermal conductivity channels between MPCM particles, boosting thermal conductivity (Figure 7). Furthermore, the phenomenon of the reduction in apparent thermal conductivity of the MPCM slurry during the phase transition interval remains substantially intact with the addition of MWCNTs, and the temperature drop area remains between 16.8 °C and 31.8 °C.

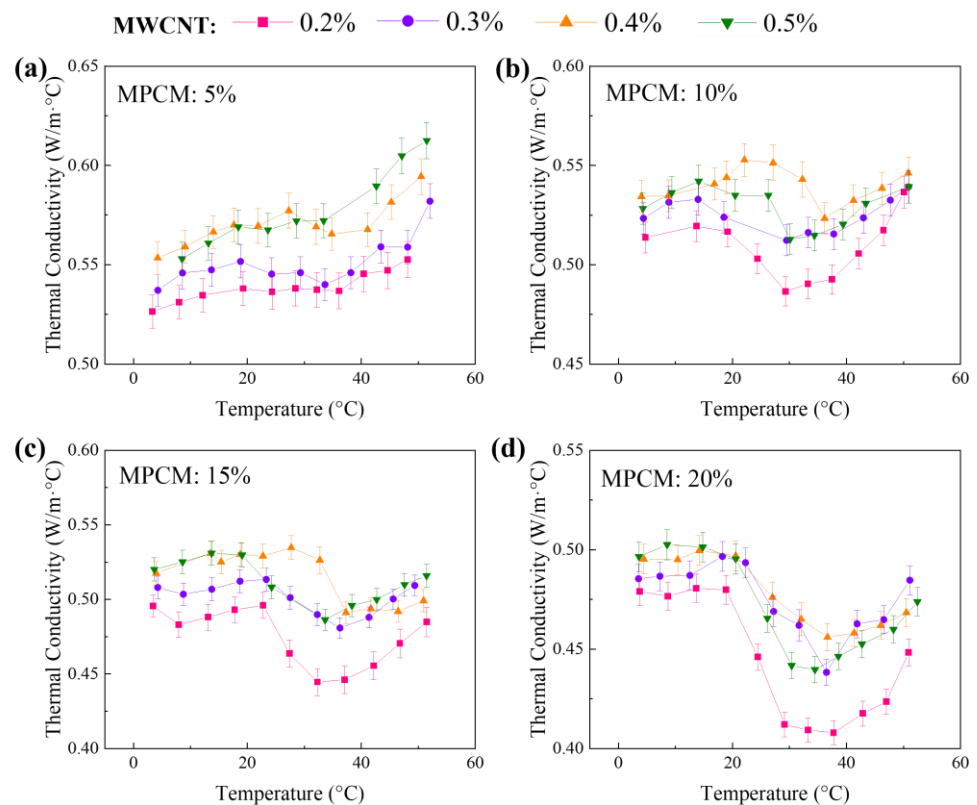


Figure 6. Thermal conductivity of MPCM slurry with different MWCNTs: (a) 5%MPCM, (b) 10%MPCM, (c) 15% MPCM, and (d) 20% MPCM slurry.

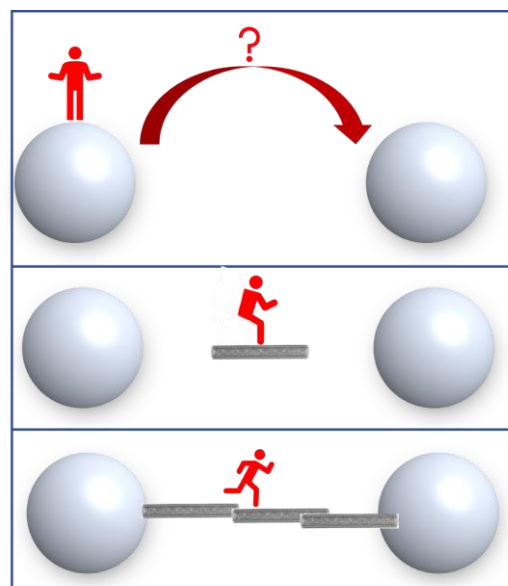


Figure 7. Mechanism diagram of thermal conductivity enhancement.

Viscosity is a crucial parameter for fluids, and the viscosity of the MPCM, MWCNTs, and their mixes was measured using a digital viscometer at 300 K. Figure 8 shows the results. The viscosity of the MWCNT dispersion can be shown to be approximately 0.9 mPa·s, which does not alter with the amount of MWCNTs added (Figure 8a). This is mostly owing to the tiny size of the additional MWCNTs, and its viscosity after the uniform dispersion is essentially equivalent to that of water. Figure 8b demonstrates a considerable variation in MPCM slurry viscosity. The viscosity increases as the mass fraction of the MPCM increases.

The rise in viscosity between 5% and 15% is not large, increasing just from 1.59 mPa·s to 11.06 mPa·s, but it jumps to 70.55 mPa·s at 20%. As seen in Figure 8c, with the addition of MWCNTs to the MPCM, the shifting pattern of viscosity becomes more complicated. The viscosity of the samples increases to a limited amount after the addition of MWCNTs to the low-concentration MPCM slurry (5% and 10%). The viscosity of the 5% MPCM slurry, for example, rises from 1.59 mPa·s to about 3.0 mPa·s with the addition of 0.5% MWCNTs. For high MPCM concentrations, such as the 20% MPCM slurry, each 0.1% increase in MWCNT addition raises the sample viscosity by 500 mPa·s to over 1000 mPa·s. The viscosity of the combination approaches 3200 mPa·s at 0.5% MWCNTs, a high viscosity that is essentially unsuitable for flow heat transfer applications due to severe flow resistance. Figure 8d illustrates the viscosity properties and variation patterns of the MWCNT-MPCM. In the diagram, the grey arcs with arrows represent the rotor running during the viscosity measurement. Because of their nanoscale size, the evenly dispersed MWCNTs in water has a modest influence on viscosity at low concentrations, nearing water viscosity. As shown in Figure 8d, the additional rise in flow shear resistance of the MPCM slurry may be generated mostly by the sticking and collision of MPCM particles inside it. After MWCNTs are introduced, the nanomaterials are engaged in mutual collisions and friction between MPCM particles, which may result in an increase in equivalent surface roughness. In addition, assuming that the MWCNTs and MPCM particles are linked in a fluffy manner, the aggregation of particles into clusters considered can also increase the viscosity. Figure 8e shows the loss of regularity in the change in viscosity with a change in rotational speed. This loss of regularity is indeed demonstrated in the experimental data, and it is speculated that this may be due to either the high concentration of the MWCNT-MPCM slurry losing some of the viscosity properties of a Newtonian fluid while not being a non-Newtonian fluid in the full sense of the word, or to the increased adhesion of the MPCM slurry to the rotor with the addition of MWCNTs, resulting in a change in the fluid's apparent viscosity varied.

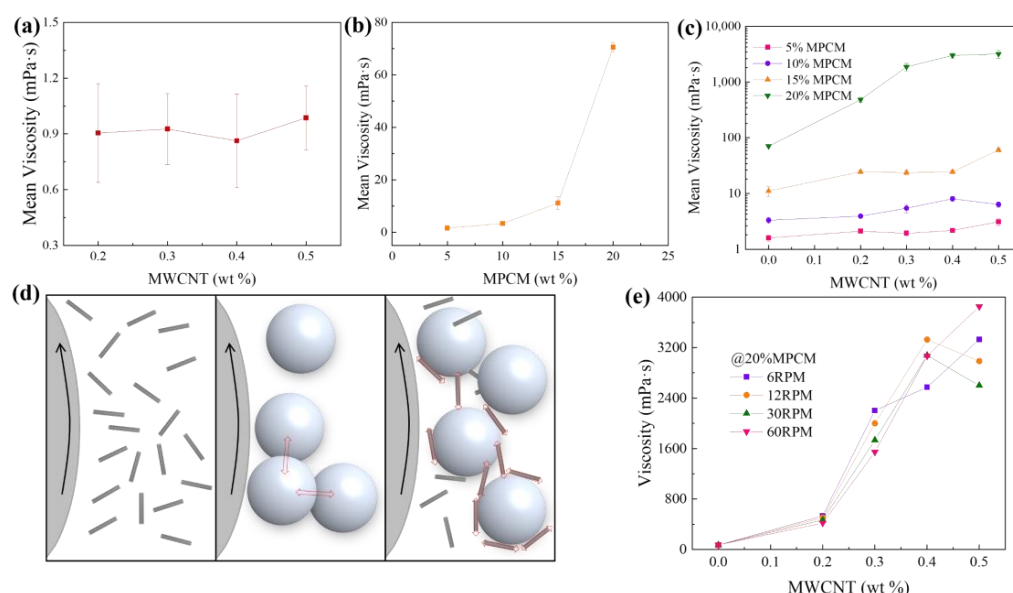


Figure 8. Mean viscosity of (a) MWCNT slurry, (b) MCPM slurry, and (c) MWCNT-MPCM slurry; (d) mechanism of increasing viscosity; (e) viscosity of MWCNT-MPCM in different rotational speed.

Photothermal conversion experiments of the hybrid MWCNT-MPCM were carried out using a solar simulator. During the test, the intensity of solar irradiation was kept constant for one sun. Figure 9 depicts the change in MPCM slurry temperature during the test. The temperature of the MPCM rises with time owing to solar irradiation absorption, and there is a noticeable temperature plateau at about 35 °C. The higher the concentration of the MPCM, the longer this temperature plateau lasts. At this temperature plateau, the

solar energy received by the material triggers a phase transition in the microcapsule core material n-icosane, allowing photothermal conversion and storage to be integrated. The addition of MWCNTs enhances the photothermal conversion rate, which accelerates the temperature rise of the MPCM slurry mixture and improves its maximum temperature. It can be shown that the enhancement of photothermal conversion at lower concentrations of MWCNTs is not considerable, and the temperature change throughout the test is not significantly different. The heat collection performance is greatly boosted following the addition of MWCNTs to 0.5%. The maximum heat collection temperature could reach 60 °C with the 5% MPCM slurry containing 0.5% MWCNTs as an example. As the MPCM content grows, the maximum temperature that the combination can achieve decreases, and the MPCM with a 20% percentage can only reach 50 °C. This temperature is, of course, enough for purposes such as supplementary building heating.

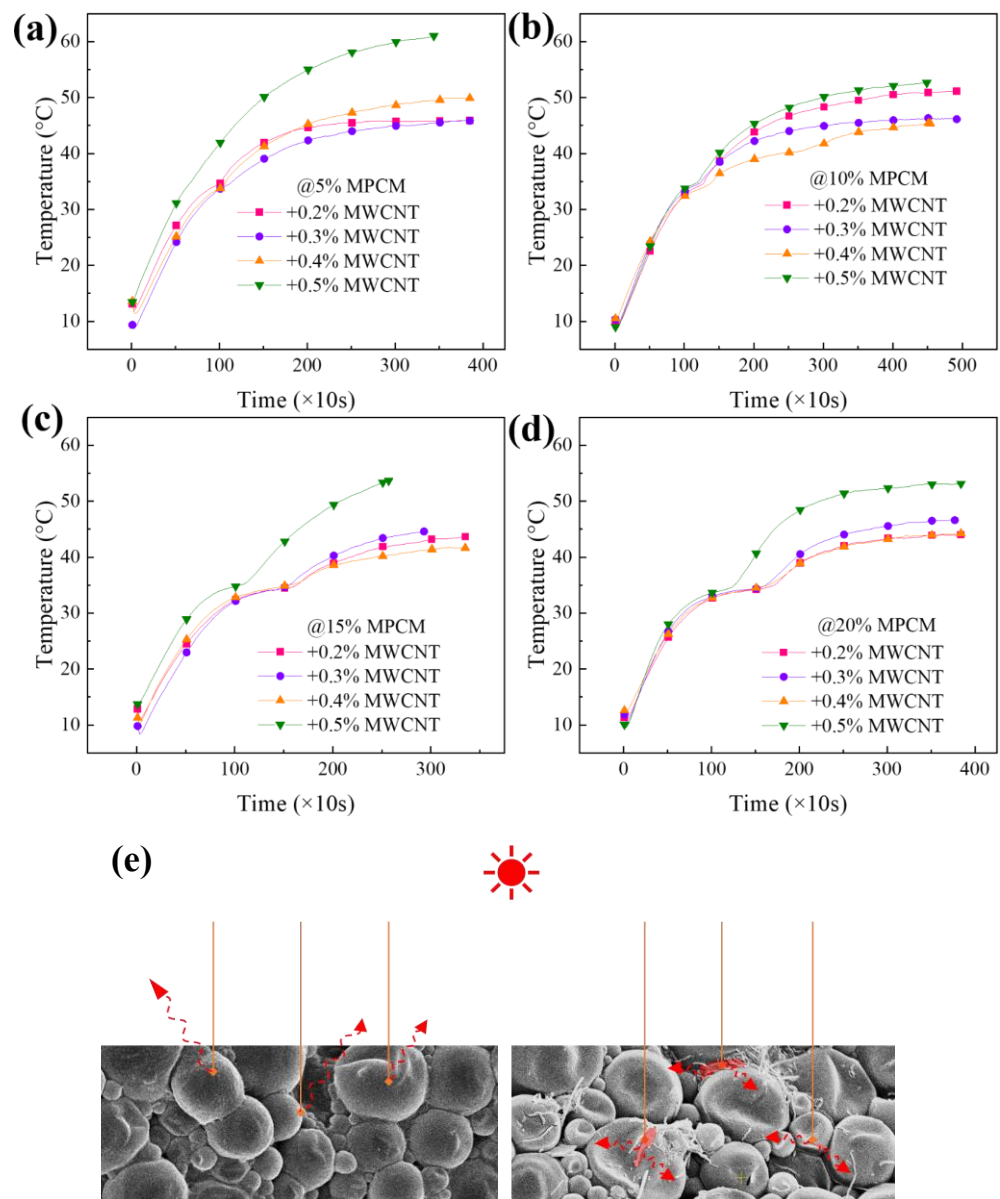


Figure 9. Photothermal performance of MPCM slurry with different MWCNTs: (a) 5%MPCM, (b) 10%MPCM, (c) 15% MPCM, and (d) 20% MPCM slurry; (e) diagram of the photothermal performance enhancement mechanism.

Figure 9e depicts the explanation by which the addition of MWCNTs aids in the photothermal conversion of the MPCM. When solar radiation reaches the MPCM without the MWCNTs, the majority of it is reflected, with the possible exception of a tiny percentage that is absorbed and transformed into heat. The MWCNTs are dispersed on the surface and are surrounding the phase change microcapsules after being introduced. The light is absorbed by the MWCNTs, and heat is transported to the MPCM due to the MWCNT's high thermal conductivity, boosting the photothermal conversion effect.

In investigating further the photothermal conversion performance, the photothermal conversion efficiency of the samples was calculated using Equation (1):

$$\eta = \frac{m\Delta H}{IA(t_e - t_s)} \quad (1)$$

where η is the photothermal conversion efficiency, m is the sample mass, ΔH is the latent heat of phase change of the sample, I is the irradiance intensity, A is the light receiving area, and t_e and t_s are the end time and start time of the phase change, respectively.

The nanotubes-enhanced photothermal conversion is dependent on the MWCNT concentration, and when the concentration is insufficient, the MWCNTs absorb part of the light but still reflect some of the solar energy. This hypothesis is supported by the fact that the low concentration of MWCNTs does not significantly improve photothermal conversion in Figure 9. It can be seen from Equation (1) that when the MPCM is added in the same amount, the sample mass m is the same and, therefore, the relative magnitude of the photothermal conversion efficiency is determined by the duration of the phase change process ($t_e - t_s$). The shorter the duration of the phase change process, the more photothermal energy is absorbed per unit of time and the higher the photothermal conversion efficiency. Using the MPCM content of 20% as an example, the photothermal conversion efficiencies of 62.99%, 64.16%, 55.6%, and 92.4% are observed for the MWCNT contents of 0.2%, 0.3%, 0.4%, and 0.5% respectively. In addition, this finding is compatible with the explanation of the mechanism for enhanced photothermal conversion efficiency shown in Figure 9.

4. Conclusions

In this work, we successfully prepared a MPCM utilizing in situ polymerization using MF as the shell material and *n*-eicosane as the core material. The thermophysical and photothermal conversion performance of the MPCM slurry were enhanced by the addition of MWCNTs. SEM images revealed that the MPCM was well structured and regularly rounded, with particle sizes ranging from 1 to 4 μm . The phase change temperature of the MPCM was 36 $^{\circ}\text{C}$, and the latent heat of phase change was 135.92 kJ/kg, according to DSC data. The addition of MWCNTs had a little influence on the material's phase transition characteristics. Viscosity experiments showed that the introduction of MWCNTs increased the viscosity of the MPCM slurry. The addition of 0.5% MWCNTs to 20% MPCM resulted in a viscosity of 3200 mPa·s, making this ratio unsuitable for use in flow heat transfer applications. More importantly, the inclusion of MWCNTs enhanced the MPCM's thermal conductivity and photothermal conversion properties. The MPCM slurry with MWCNTs had a thermal conductivity of up to 0.6 W/m· $^{\circ}\text{C}$. The highest heat collecting temperature of the MWCNT-MPCM slurry under a simulated solar intensity of 1 sun was up to 60 $^{\circ}\text{C}$, and the maximum photothermal conversion efficiency was up to 92.4%. As a result of its excellent thermal storage performance and good photothermal conversion efficiency, the MWCNT-MPCM slurry has a promising future in solar thermal utilization and thermal storage.

Author Contributions: Conceptualization, X.Z. and C.W.; investigation, C.W. and G.Z.; writing—original draft preparation, C.W.; writing—review and editing, C.W.; visualization, C.W.; supervision, X.Z.; funding acquisition, X.Z. All authors have read and agreed to the published version of the manuscript.

Funding: This research was funded by the National Natural Science Foundation of China (No. 51876034).

Data Availability Statement: Not applicable.

Conflicts of Interest: The authors declare no conflict of interest.

References

1. Paul, J.; Kadirgama, K.; Samykano, M.; Pandey, A.K.; Tyagi, V.V. A comprehensive review on thermophysical properties and solar thermal applications of organic nano composite phase change materials. *J. Energy Storage* **2022**, *45*, 103415. [[CrossRef](#)]
2. Robertson, N. Catching the rainbow: Light harvesting in dye-sensitized solar cells. *Angew. Chem. Int. Ed.* **2008**, *47*, 1012–1014. [[CrossRef](#)]
3. Zhao, J.; Zhou, J.; Li, H.; Li, X. Cuprous oxide modified nanoencapsulated phase change materials fabricated by RAFT miniemulsion polymerization for thermal energy storage and photothermal conversion. *Powder Technol.* **2022**, *399*, 117189. [[CrossRef](#)]
4. Zhang, X.; Zhang, Y.; Yan, Y.; Chen, Z. Synthesis and characterization of hydroxylated carbon nanotubes modified microencapsulated phase change materials with high latent heat and thermal conductivity for solar energy storage. *Sol. Energy Sol. Cells* **2022**, *236*, 111546. [[CrossRef](#)]
5. Yu, C.; Park, J.; Youn, J.R.; Song, Y.S. Sustainable solar energy harvesting using phase change material (PCM) embedded pyroelectric system. *Energy Convers. Manag.* **2022**, *253*, 115145. [[CrossRef](#)]
6. Yan, D.; Li, M. TaON doped metal-organic frameworks-based composite phase change materials with excellent photo-thermal conversion performance. *Sol. Energy Mater. Sol. Cells* **2022**, *243*, 111790. [[CrossRef](#)]
7. Sun, Z.; Shi, T.; Wang, Y.; Li, J.; Liu, H.; Wang, X. Hierarchical microencapsulation of phase change material with carbon-nanotubes/polydopamine/silica shell for synergistic enhancement of solar photothermal conversion and storage. *Sol. Energy Mater. Sol. Cells* **2022**, *236*, 111539. [[CrossRef](#)]
8. Wang, X.; Gao, Y.; Han, N.; Zhang, X.; Li, W. Design and synthesis of microcapsules with cross-linking network supporting core for supercooling degree regulation. *Energy Build.* **2021**, *253*, 111437. [[CrossRef](#)]
9. Qin, M.; Feaugas, O.; Zu, K. Novel metal-organic framework (MOF) based phase change material composite and its impact on building energy consumption. *Energy Build.* **2022**, *273*, 112382. [[CrossRef](#)]
10. Yuan, S.; Yan, R.; Ren, B.; Du, Z.; Cheng, X.; Du, X.; Wang, H. Robust, double-layered phase-changing microcapsules with superior solar-thermal conversion capability and extremely high energy storage density for efficient solar energy storage. *Renew. Energy* **2021**, *180*, 725–733. [[CrossRef](#)]
11. Al-Shannaq, R.; Farid, M.; Al-Muhtaseb, S.; Kurdi, J. Emulsion stability and cross-linking of PMMA microcapsules containing phase change materials. *Sol. Energy Mater. Sol. Cells* **2015**, *132*, 311–318. [[CrossRef](#)]
12. Sun, J.; Zhao, J.; Wang, B.; Li, Y.; Zhang, W.; Zhou, J.; Guo, H.; Liu, Y. Biodegradable wood plastic composites with phase change microcapsules of honeycomb-BN-layer for photothermal energy conversion and storage. *Chem. Eng. J.* **2022**, *448*, 137218. [[CrossRef](#)]
13. Chen, X.; Kong, X.; Wang, S.; Fu, X.; Yu, B.; Yao, K.; Zhong, Y.; Li, J.; Xu, W.; Liu, Y. Microencapsulated phase change materials: Facile preparation and application in building energy conservation. *J. Energy Storage* **2022**, *48*, 104025. [[CrossRef](#)]
14. Zhu, X.; Sheng, X.; Li, J.; Chen, Y. Thermal comfort and energy saving of novel heat-storage coatings with microencapsulated PCM and their application. *Energy Build.* **2021**, *251*, 111349. [[CrossRef](#)]
15. Yang, R.; Li, D.; Salazar, S.L.; Rao, Z.; Arıcı, M.; Wei, W. Photothermal properties and photothermal conversion performance of nano-enhanced paraffin as a phase change thermal energy storage material. *Sol. Energy Mater. Sol. Cells* **2021**, *219*, 110792. [[CrossRef](#)]
16. Ma, X.; Liu, H.; Chen, C.; Liu, Y.; Zhang, L.; Xu, B.; Xiao, F. Synthesis of novel microencapsulated phase change material with SnO₂/CNTs shell for solar energy storage and photo-thermal conversion. *Mater. Res. Express* **2020**, *7*, 015513. [[CrossRef](#)]
17. Gao, G.; Zhang, T.; Jiao, S.; Guo, C. Preparation of reduced graphene oxide modified magnetic phase change microcapsules and their application in direct absorption solar collector. *Sol. Energy Mater. Sol. Cells* **2020**, *216*, 110695. [[CrossRef](#)]
18. Meng, D.; Yang, S.; Guo, L.; Li, G.; Ge, J.; Huang, Y.; Bielawski, C.W.; Geng, J. The enhanced photothermal effect of graphene/conjugated polymer composites: Photoinduced energy transfer and applications in photocontrolled switches. *Chem. Commun.* **2014**, *50*, 14345–14348. [[CrossRef](#)]
19. Xu, B.; Wei, Z.; Hong, X.; Zhou, Y.; Gan, S.; Shen, M. Preparation and characterization of novel microencapsulated phase change materials with SiO₂/FeOOH as the shell for heat energy storage and photocatalysis. *J. Energy Storage* **2021**, *43*, 103251. [[CrossRef](#)]
20. Lin, J.; Ouyang, Y.; Chen, L.; Wen, K.; Li, Y.; Mu, H.; Ren, Q.; Xie, X.; Long, J. Enhancing the solar absorption capacity of expanded graphite-paraffin wax composite phase change materials by introducing carbon nanotubes additives. *Surf. Interfaces* **2022**, *30*, 101871. [[CrossRef](#)]
21. Zheng, X.; Gao, X.; Huang, Z.; Li, Z.; Fang, Y.; Zhang, Z. Form-stable paraffin/graphene aerogel/copper foam composite phase change material for solar energy conversion and storage. *Sol. Energy Mater. Sol. Cells* **2021**, *226*, 111083. [[CrossRef](#)]
22. Maithya, O.M.; Li, X.; Feng, X.; Sui, X.; Wang, B. Microencapsulated phase change material via Pickering emulsion stabilized by graphene oxide for photothermal conversion. *J. Mater. Sci.* **2020**, *55*, 7731–7742. [[CrossRef](#)]
23. Maithya, O.M.; Zhu, X.; Li, X.; Korir, S.J.; Feng, X.; Sui, X.; Wang, B. High-energy storage graphene oxide modified phase change microcapsules from regenerated chitin Pickering Emulsion for photothermal conversion. *Sol. Energy Mater. Sol. Cells* **2021**, *222*, 110924. [[CrossRef](#)]

24. Zhao, Q.; He, F.; Zhang, Q.; Fan, J.; He, R.; Zhang, K.; Yan, H.; Yang, W. Microencapsulated phase change materials based on graphene Pickering emulsion for light-to-thermal energy conversion and management. *Sol. Energy Mater. Sol. Cells* **2019**, *203*, 110204. [[CrossRef](#)]
25. Liu, H.; Tian, X.; Ouyang, M.; Wang, X.; Wu, D.; Wang, X. Microencapsulating n-docosane phase change material into $\text{CaCO}_3/\text{Fe}_3\text{O}_4$ composites for high-efficient utilization of solar photothermal energy. *Renew. Energy* **2021**, *179*, 47–64. [[CrossRef](#)]
26. Fan, X.; Qiu, X.; Lu, L.; Zhou, B. Full-spectrum light-driven phase change microcapsules modified by CuS-GO nanoconverter for enhancing solar energy conversion and storage capability. *Sol. Energy Mater. Sol. Cells* **2021**, *223*, 110937. [[CrossRef](#)]
27. Eisapour, M.; Eisapour, A.H.; Hosseini, M.J.; Talebizadehsardari, P. Exergy and energy analysis of wavy tubes photovoltaic-thermal systems using microencapsulated PCM nano-slurry coolant fluid. *Appl. Energy* **2020**, *266*, 114849. [[CrossRef](#)]
28. Ho, C.J.; Tanuwijaya, A.O.; Lai, C.-M. Thermal and electrical performance of a BIPV integrated with a microencapsulated phase change material layer. *Energy Build.* **2012**, *50*, 331–338. [[CrossRef](#)]
29. Liu, L.; Jia, Y.; Lin, Y.; Alva, G.; Fang, G. Performance evaluation of a novel solar photovoltaic–thermal collector with dual channel using microencapsulated phase change slurry as cooling fluid. *Energy Convers. Manag.* **2017**, *145*, 30–40. [[CrossRef](#)]
30. Liu, L.; Jia, Y.; Lin, Y.; Alva, G.; Fang, G. Numerical study of a novel miniature compound parabolic concentrating photovoltaic/thermal collector with microencapsulated phase change slurry. *Energy Convers. Manag.* **2017**, *153*, 106–114. [[CrossRef](#)]
31. Moradi, H.; Mirjalily, S.A.A.; Oloomi, S.A.A.; Karimi, H. Performance evaluation of a solar air heating system integrated with a phase change materials energy storage tank for efficient thermal energy storage and management. *Renew. Energy* **2022**, *191*, 974–986. [[CrossRef](#)]
32. Hu, D.; Han, L.; Zhou, W.; Li, P.; Huang, Y.; Yang, Z.; Jia, X. Flexible phase change composite based on loading paraffin into cross-linked CNT/SBS network for thermal management and thermal storage. *Chem. Eng. J.* **2022**, *437*, 135056. [[CrossRef](#)]
33. Atinafu, D.G.; Wi, S.; Yun, B.Y.; Kim, S. Engineering biochar with multiwalled carbon nanotube for efficient phase change material encapsulation and thermal energy storage. *Energy* **2021**, *216*, 119294. [[CrossRef](#)]
34. Ong, P.J.; Png, Z.M.; Soo, X.Y.D.; Wang, X.; Suwardi, A.; Chua, M.H.; Xu, J.W.; Zhu, Q. Surface modification of microencapsulated phase change materials with nanostructures for enhancement of their thermal conductivity. *Mater. Chem. Phys.* **2022**, *277*, 125438. [[CrossRef](#)]
35. Khudhair, A.M.; Farid, M.M. A review on energy conservation in building applications with thermal storage by latent heat using phase change materials. *Energy Convers. Manag.* **2004**, *45*, 263–275. [[CrossRef](#)]
36. Tyagi, V.V.; Kaushik, S.C.; Tyagi, S.K.; Akiyama, T. Development of phase change materials based microencapsulated technology for buildings: A review. *Renew. Sustain. Energy Rev.* **2011**, *15*, 1373–1391. [[CrossRef](#)]
37. Giro-Paloma, J.; Martínez, M.; Cabeza, L.F.; Fernández, A.I. Types, methods, techniques, and applications for microencapsulated phase change materials (MPCM): A review. *Renew. Sustain. Energy Rev.* **2016**, *53*, 1059–1075. [[CrossRef](#)]
38. Yu, Q.; Chen, X.; Yang, H. Research progress on utilization of phase change materials in photovoltaic/thermal systems: A critical review. *Renew. Sustain. Energy Rev.* **2021**, *149*, 111313. [[CrossRef](#)]
39. Tang, Z.; Gao, H.; Chen, X.; Zhang, Y.; Li, A.; Wang, G. Advanced multifunctional composite phase change materials based on photo-responsive materials. *Nano Energy* **2021**, *80*, 105454. [[CrossRef](#)]
40. Li, M.; Mu, B. Effect of different dimensional carbon materials on the properties and application of phase change materials: A review. *Appl. Energy* **2019**, *242*, 695–715. [[CrossRef](#)]
41. Liu, H.; Wang, X.; Wu, D. Innovative design of microencapsulated phase change materials for thermal energy storage and versatile applications: A review. *Sustain. Energy Fuels* **2019**, *3*, 1091–1149. [[CrossRef](#)]
42. Su, W.; Hu, M.; Wang, L.; Kokogiannakis, G.; Chen, J.; Gao, L.; Li, A.; Xu, C. Microencapsulated phase change materials with graphene-based materials: Fabrication, characterisation and prospects. *Renew. Sustain. Energy Rev.* **2022**, *168*, 112806. [[CrossRef](#)]
43. Rodríguez-Cumplido, F.; Pabón-Gelves, E.; Chejne-Jana, F. Recent developments in the synthesis of microencapsulated and nanoencapsulated phase change materials. *J. Energy Storage* **2019**, *24*, 100821. [[CrossRef](#)]